International Journal of Microwave and Wireless Technologies, 2017, 9(2), 275–280.
doi:10.1017/S1759078715001695

RESEARCH PAPER

Theoretical study of liquid crystal dielectric-loaded plasmonic waveguide

HAMED ARMAND[1] AND M. DASHTI ARDAKANI[2]

A fully two-dimensional theoretical study of the electromagnetic wave propagation through Metal–Liquid Crystal–Metal (M–LC–M) waveguide structure is presented. Dispersion relations corresponding to both symmetric and antisymmetric-coupled surface plasmons polaritons modes in M–LC–M structure are derived and numerically solved. The effects of LC tilt angles on the effective refractive index and propagation length are proposed. The analytical method is in good agreement with those obtained from finite-difference time-domain simulation. The obtained analytic formula can be used as an efficient element in designing tunable ultrahigh nanoscale integrated plasmonic devices.

Keywords: Plasmonic, Surface plasmons, Liquid crystal, FDTD

Received 16 August 2015; Revised 28 October 2015; Accepted 5 November 2015; first published online 7 December 2015

I. INTRODUCTION

Recent researches in plasmonics areas have led to important progress in development of various metal–insulator–metal (MIM) plasmonic devices. Plasmonic studies have almost exclusively focused on pure metallic nanostructures and passive components with properties fixed by the nanostructure structural parameters. As the greatest challenge, real-life applications require active control of plasmonic signals in nano-optic devices [1, 2]. Moreover, it is advantageous to be able to tune plasmonic passive devices. All these can be realized if plasmonic nanostructures are hybridized with functional materials. Development of electro-optical materials and integrating them with plasmonic nanostructures, give rise to great research effort in proposing active plasmonic devices [3]. Electro-optic control of plasmonic signals can be provided by the use of nematic LC (N-LC). N-LC, because of high levels of controllable birefringence, supports the external manipulation of plasmonic signals via external electric fields. Recently, LC thin films with a thickness of a few nanometers have attracted much interest due to their relaxation time of less than a nanosecond [4]. There has been concerted research to investigate the properties of thin LC layers both theoretically and experimentally [5–7]. With its low driving voltage and low-cost fabrication technology, LC technology seems to be an outstanding candidate for tunable plasmonic devices and is proposed for various applications [8–10].

In order to design plasmonic devices, it is necessary to derive the dispersion relation of the desirable structure. Anisotropic behavior of the LC affects the propagation of surface plasmons polaritons (SPPs), and makes the inclusion of anisotropy in the theory inevitable. The existence of transverse magnetic (TM) modes at the interface of an anisotropic uniaxial dielectric and a metal has been discussed in [11, 12]. However, these works have been restricted to materials with diagonal dielectric tensors, and the resulting equations are nearly identical to those used in the original isotropic media. A simplified theoretical study of electromagnetic wave propagation through insulator–metal–insulator and MIM structures consisting of anisotropic dielectric layers with off-diagonal dielectric tensor has performed [13]. However, the principal axes of the anisotropic slab are simply chosen parallel to the metal/anisotropic interface and the directions of the electromagnetic fields are chosen in a manner which the electric field vector is in parallel with electric flux density. In a recent work, the guided optical modes of a planar plasmonic waveguide filled with a generic anisotropic medium have been studied [14].

However, previous works on the fundamental guided dispersion characteristics are still incomplete. In particular, discussions related to the electro-optic control of plasmonic signals are insufficient, which can be significant design guidelines for active plasmonic devices. Dispersion relation of LC dielectric-loaded MIM waveguides has not been extracted yet and there is not any deep analysis of this structure in the previous literatures. In this paper, we propose a hybrid plasmonic nanostructure consisting of nanostructured metals combined with LCs to enable active functionalities in plasmonic circuitry. The dispersion relations corresponding to both symmetric and antisymmetric modes in the metal–liquid crystal–metal (M–LC–M) structure are derived without any approximation and numerically solved. The motivation for considering LC is the possibility of utilizing the LC parameters in controlling the plasmonic signals. Our results have some potential application in designing tunable compact nanophotonic devices.

[1]Department of Electrical and Computer Engineering, K. N. Toosi University of Technology, Tehran, Iran.
[2]Department of Electrical Engineering, Iran University of Science and Technology, Tehran, Iran. Phone: +98 913 359 4943
Corresponding author:
M. Dashti Ardakani
Email: mansoor.dashti@gmail.com

II. GENERAL DISPERSION RELATION OF M-LC-M STRUCTURE

The structure under study, shown in Fig. 1, comprises a slab of thickness $2a$ with its interfaces orthogonal to the x-axis, filled with N-LC and sandwiched between two silver layers. Dispersive behavior of silver is estimated using Drude model. This structure acts as a waveguide for the SPP propagating along the z-direction in the form of a waveguide mode for the TM-polarized case. To consider only excitation of the fundamental SPP mode, the width of the LC layer is chosen to be much smaller than the wavelength of incident light. In general anisotropic media, the properties of the medium are expressed in tensor form. In this paper, we assume that our structure is only electrically anisotropic. Assuming the optical axis of the anisotropic molecules in the X–Z-plane, the dielectric tensor of the LC medium is given by [10]:

$$\bar{\bar{\varepsilon}} = \begin{bmatrix} n_e^2\cos^2\theta + n_o^2\sin^2\theta n & 0 & \left(n_e^2 - n_o^2\right)\sin\theta\cos\theta \\ 0 & n_e^2 & 0 \\ \left(n_e^2 - n_o^2\right)\sin\theta\cos\theta & 0 & n_o^2\cos^2\theta + n_e^2\sin^2\theta \end{bmatrix}, \tag{1}$$

where n_o and n_e are the ordinary and extraordinary indices of refraction, respectively. In the equations above, θ, called tilt angle, is the angle between the optical axis of the anisotropic molecules and the z-direction. In the entire paper, n_e and n_o are considered to be 1.737 and 1.518, respectively, which belong to a positive N-LC ($E7$) at room temperature.

The amount of voltage needed to switch an N-LC modulator is a function of the specific material used, cell thickness, and alignment. Our device takes advantage of the metallic nature of the structure, where the metal walls can serve as electrodes. A low-frequency voltage of varying value is applied at the upper silver layer; the electrical path terminates at the lower metal film, which is grounded. The electric field induces a reorientation of the LC molecules, which tend to align with the applied field, modifying the overall electrical and subsequently optical properties of the LC material. The exact profile of the molecular orientations and the extent of the LC-switching depend on the value of the applied voltage, the molecular anchoring conditions at the walls, the geometry of the structure, and the material properties of the LC and the surrounding isotropic materials. As the applied voltage increases, the tilt angle of each molecule increases because the LC molecules tend to align with the electric field. For a sufficiently high voltage, the strong electric field inside the waveguide plays a significant role in the LC-orientation behavior. Because of nanometer-sized waveguide, the electric field inside the waveguide is strong enough to switch all the nematic molecules; and the strong electric field dominates the anchoring condition at the M–LC interface. Thus, the LC is considered to be fully switched, when the nematic director of the material tends to align in parallel to the x-axis, so that the tilt angles of the molecules in this area all approximate 90°. Hence, good alignment quality and device switching can be achieved.

To obtain the dispersion relation, we first derive the wave equation inside the LC medium. Just the TM condition is considered. For propagation along the z-direction and homogeneity in the y-direction, propagation of the magnetic field in LC medium is described as follows:

$$\nabla \times H = \begin{vmatrix} \hat{a}_x & \hat{a}_y & \hat{a}_z \\ \frac{\partial}{\partial x} & 0 & j\beta_z \\ H_x & H_y & H_z \end{vmatrix} = j\omega\bar{\bar{\varepsilon}}E, \tag{2}$$

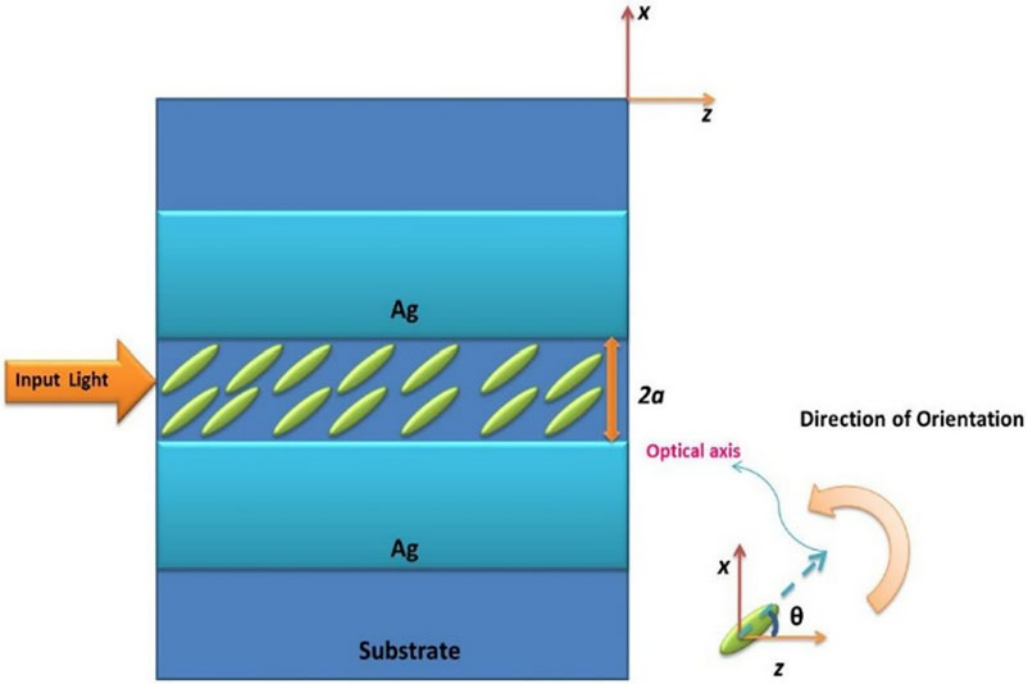

Fig. 1. General Schematic of the M–LC–M waveguide structure [15].

https://doi.org/10.1017/S1759078715001695 Published online by Cambridge University Press

$$\frac{1}{j\omega}\overline{\overline{\eta}}\begin{pmatrix} -j\beta_z H_y \\ -j\beta_z H_x - \dfrac{\partial H_z}{\partial x} \\ \dfrac{\partial H_y}{\partial x} \end{pmatrix} = \begin{pmatrix} E_x \\ E_y \\ E_z \end{pmatrix}, \tag{3}$$

$$\frac{1}{j\omega}\begin{pmatrix} \eta_{xx} & 0 & \eta_{xz} \\ 0 & \eta_{yy} & 0 \\ \eta_{zx} & 0 & \eta_{zz} \end{pmatrix}\begin{pmatrix} -j\beta_z H_y \\ -j\beta_z H_x - \dfrac{\partial H_z}{\partial x} \\ \dfrac{\partial H_y}{\partial x} \end{pmatrix} = \begin{pmatrix} E_x \\ E_y \\ E_z \end{pmatrix}, \tag{4}$$

$$E_x = \frac{1}{j\omega}\left[\eta_{xx}(-j\beta_z H_y) + \eta_{xz}\left(\frac{\partial H_y}{\partial x}\right)\right], \tag{5}$$

$$E_z = \frac{1}{j\omega}\left[\eta_{zx}(-j\beta_z H_y) + \eta_{zz}\left(\frac{\partial H_y}{\partial x}\right)\right], \tag{6}$$

$$\nabla \times E = \begin{vmatrix} \hat{a}_x & \hat{a}_y & \hat{a}_z \\ \dfrac{\partial}{\partial x} & 0 & j\beta_z \\ E_x & E_y & E_z \end{vmatrix} = -j\omega\mu H = -j\omega\mu\begin{pmatrix} H_x \\ H_y \\ H_z \end{pmatrix}, \tag{7}$$

$$\frac{\partial E_z}{\partial x} - j\beta_z E_x = j\omega\mu H_y, \tag{8}$$

$$\frac{\partial^2 H_y}{\partial x^2} - 2j\beta_z \frac{\eta_{xz}}{\eta_{zz}}\frac{\partial H_y}{\partial x} - \left(\beta_z^2 \frac{\eta_{xx}}{\eta_{zz}} - \frac{\omega^2 \mu_o}{\eta_{zz}}\right)H_y = 0, \tag{9}$$

where η is the impermeability tensor of the LC layer. Practically, equation (9) has to be solved in the LC region, and the obtained solution has to be matched with the solution of wave equation inside plasmonic regions using appropriate boundary conditions. The wave equation and also the field components for TM modes inside the plasmonic regions ($x > a$ and $x < -a$) is provided in [16]. In the core region, $-a < x < a$, the modes localized at the bottom and the top interface couple, yielding

$$H_y = \left(e^{j\beta_x x}e^{k_d x} \pm e^{j\beta_x x}e^{-k_d x}\right)e^{j\beta_z z}, \tag{10}$$

$$E_x = \frac{1}{j\omega}\left\{\eta_{xx}\left[e^{j\beta_x x}e^{k_d x}j\beta_z \pm e^{j\beta_x x}e^{-k_d x}j\beta_z\right] - \eta_{xz}\left[\left(j\beta_x + k_d\right)e^{j\beta_x x}e^{k_d x} \pm \left(j\beta_x - k_d\right)e^{j\beta_x x}e^{-k_d x}\right]\right\}e^{j\beta_z z}, \tag{11}$$

$$E_z = \frac{1}{j\omega}\left\{\eta_{zx}\left[e^{j\beta_x x}e^{k_d x}j\beta_z \pm e^{j\beta_x x}e^{-k_d x}j\beta_z\right] - \eta_{zz}\left[\left(j\beta_x + k_d\right)e^{j\beta_x x}e^{k_d x} \pm \left(j\beta_x - k_d\right)e^{j\beta_x x}e^{-k_d x}\right]\right\}e^{j\beta_z z}, \tag{12}$$

where the "+" yields the even (symmetric) solutions and "−" yields the odd (antisymmetric) solutions. By applying boundary condition at $x = \pm a$ for Hy and Ez components, the dispersion relation for M–LC–M waveguide can be achieved:

$$\eta_{zx} j\beta_z - \eta_{zz} j\beta_x - \eta_{zz} k_d \begin{Bmatrix} \tanh(k_d a) \\ \coth(k_d a) \end{Bmatrix} = \frac{k_m}{\varepsilon_m}, \tag{13}$$

$$\beta_x = \beta_z \frac{\eta_{xz}}{\eta_{zz}}, \quad k_d = \sqrt{\beta_z^2 \frac{\eta_{xx}}{\eta_{zz}} - \frac{\omega^2 \mu_o}{\eta_{zz}} - \beta_x^2},$$
$$k_m = \sqrt{\beta_z^2 - \varepsilon_m k_o^2},$$

where β_x, k_d, and k_m are the propagation constant and attenuation constants in the transverse direction, respectively. β_z is the complex propagation in the longitudinal direction, ε_m is the dielectric constant of metal, and k_o is the free-space wave constant.

Here, the "tanh" function represents the symmetric plasmon modes and the "coth" function represents the antisymmetric modes. This dispersion relation equation can be used in design of active electro-optical plasmonic devices.

III. CHARACTERISTICS OF M-LC-M STRUCTURE

The dispersion relation is now applied to M–LC–M structure with different tilt angles in LC layer. The propagation constant β_z is represented as the effective refractive index $n_{eff} = \beta_z/k_o$ of the waveguide for SPPs. The real part of n_{eff} of the M–LC–M waveguide as a function of the waveguide width for different tilt angles is shown in Fig. 2(a). The wavelength of the input continuous wave is $\lambda = 850$ nm. It is clearly seen that for a fixed value of tilt angle, n_{eff} would decrease by increasing the waveguide width. Moreover, by increasing the tilt angle for a fixed value of waveguide width, n_{eff} would decrease. Moreover, Fig. 2(b) shows the real part of n_{eff} versus wavelength for different tilt angles. The width of the LC layer is chosen to be 100 nm. By increasing the wavelength or increasing the tilt angle, n_{eff} would decrease. It is clearly demonstrated that high light confinement can be achieved for smaller LC tilt angles in M–LC–M structure.

The imaginary part of n_{eff} is referred to the propagation length which is defined as the length over which the power carried by the wave decays to $1/e$ of its initial value: $L_{spp} = 1/[2.\mathrm{Im}(\beta_z)]$. The contour map of the propagation length of M–LC–M structure as a function of the thickness of the LC layer and tilt angle is illustrated in Fig. 3(a). The wavelength of the input signal is $\lambda = 850$ nm. As can be seen, the symmetric mode surface plasmons in M–LC–M structures exhibited a reduction in propagation length and enhanced field confinement by decreasing the LC layer thickness. Moreover, for a fixed value of LC layer thickness, the propagation length is increased by increasing the tilt angle. It is clear that the smaller tilt angle will have higher loss and shorter propagation length, although the field confinement of the M–LC–M waveguide is stronger. The propagation length varies significantly with the wavelength of the input signal for M–LC–M structures. Figure 3(b) demonstrates the contour map of the propagation length of M–LC–M structure as a function of

https://doi.org/10.1017/S1759078715001695 Published online by Cambridge University Press

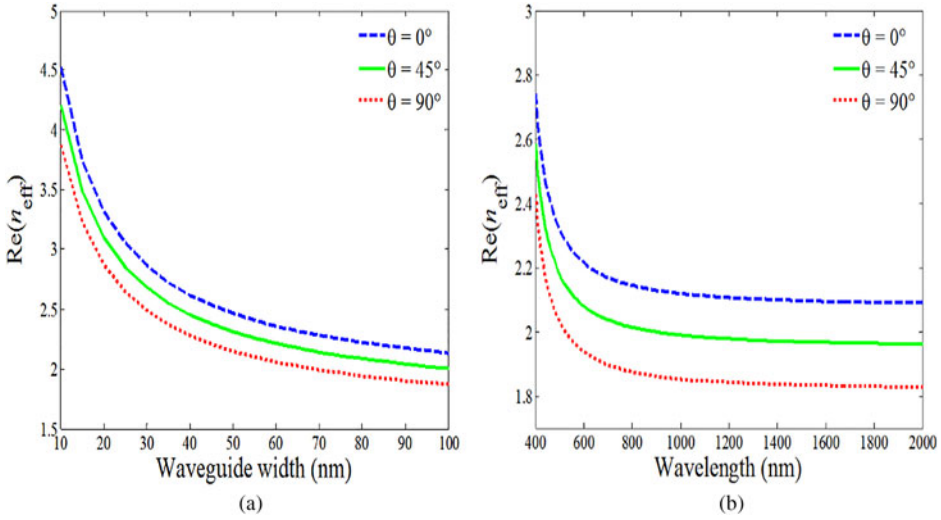

Fig. 2. The real part of n_{eff} of the M–LC–M waveguide as a function of (a) the waveguide width and (b) wavelength [17] for different tilt angles.

wavelength and tilt angle. The width of the LC layer is 100 nm. As can be seen, the propagation length increases by increasing the wavelength. Moreover, for a fixed value of wavelength, the propagation length is increased by increasing the tilt angle.

IV. VALIDATION OF THE ANALYTIC FORMULA

In order to validate our approach, the analytical results are compared with finite-difference time-domain (FDTD) calculations. A general schematic diagram of the geometry under study is shown in Fig. 4(a). The structure comprises a slit of width 100 nm sandwiched between two metal films. In our analysis, the anisotropic-dispersive FDTD (A-D–FDTD) method is employed to calculate the wavelength of SPPs. The FDTD grid size and time step are: $\Delta x = \Delta z = 1$ nm and Δt is achieved following the Courant stability condition. The structure is homogenous in the y-direction and the optical axis of the LC molecules is in the X–Z-plane [10, 18–20]. Therefore, the structure is considered as two-dimensional (2D) case. The 2D calculations agree well with full three-dimensional (3D) calculations and also the experimental results [11, 21–25]. The 2D FDTD simulation requires less computer resources than a 3D simulation. Although the amount of computation in a 3D simulation can be reduced by invoking additional symmetry considerations, in many cases, such procedures may not be enough; hence, most of the plasmonic devices can be considered as 2D structures.

At this stage, the structure is analyzed in isotropic state, i.e. it is assumed that no LC is used in the structure and the slit is filled with air. Incident light is a TM-polarized plane wave of 850 nm wavelength under the excitation condition of SPPs. In order to calculate λ_{spp} and understand the physics underlying the structure, the FDTD simulation of electric field distribution (E_z) is illustrated in Fig. 4(b). As can be seen, the SPPs excite at metal–air interfaces. λ_{spp} is defined as the distance between two adjacent positive or negative peaks.

The calculated SPP wavelength from FDTD simulation for the M–air–M structure is about 699.5 nm which is in good agreement with the corresponding value derived from analytic dispersion relation of equation (13), in isotropic case, which is

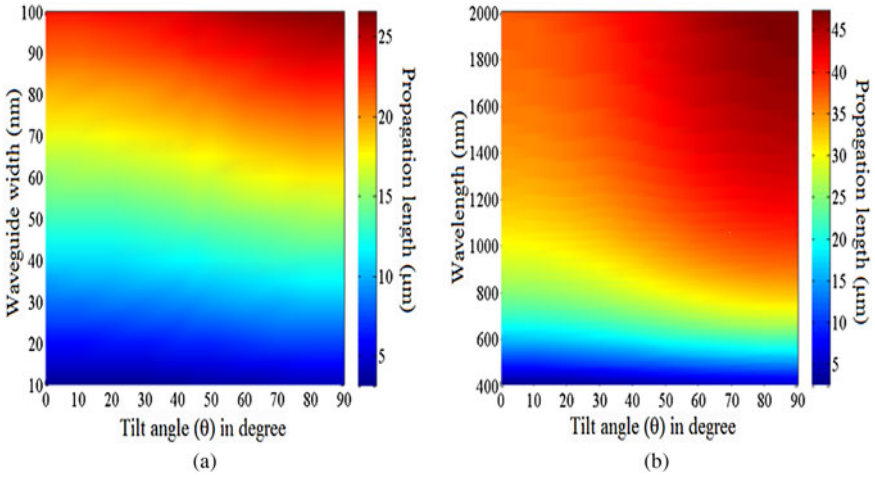

Fig. 3. Contour map of the propagation length of M–LC–M structure as a function of (a) the thickness of the LC layer and tilt angle and (b) wavelength and tilt angle.

https://doi.org/10.1017/S1759078715001695 Published online by Cambridge University Press

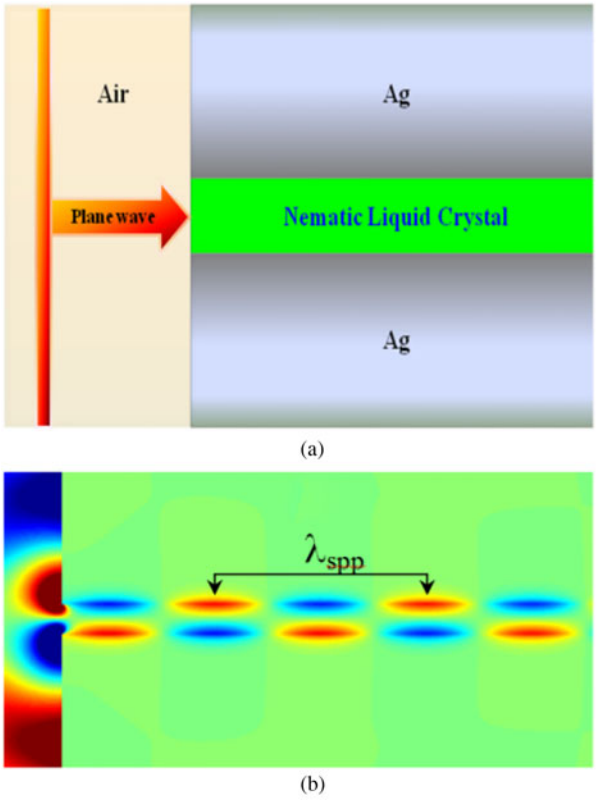

Fig. 4. (a) M–LC–M structure under study and (b) the FDTD simulation of electric field distribution (E_z) for M–air–M structure. The incident light is a TM-polarized plane wave of 850 nm wavelength.

about 700 nm. By changing the optical properties of the material inside the slit, the structure could benefit from the tunability feature. Therefore, at this stage, the slit is filled with LC. The values of λ_{spp} at different tilt angles are calculated. Changing the optical axis orientation (θ) of LC alters the effective permittivity, and thus, the optical response of the structure. Consequently, SPP wavelength can then be changed by controlling the voltage.

Figure 5 shows the comparison between our FDTD results of λ_{spp} and those obtained by analytical calculations. The comparison between our FDTD results and those obtained by analytical calculations shows qualitatively the same behavior and

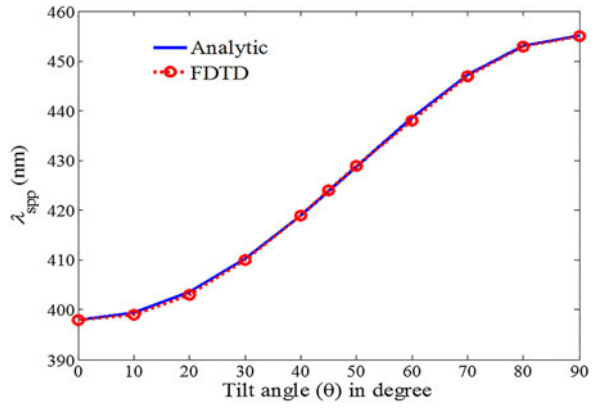

Fig. 5. The comparison between FDTD results of λ_{spp} with those obtained by analytical calculations for M–LC–M structure. The incident light is a TM-polarized plane wave of 850 nm wavelength.

clearly validate the accuracy of our analytic formula. The relative error calculated as $(|\lambda_{FDTD}-\lambda_{Analytical}|)/\lambda_{Analytical}$ does not exceed 0.12%.

V. CONCLUSION

Summarizing, we theoretically investigated the behavior of electromagnetic waves in M–LC–M structure. Dispersion relations corresponding to both symmetric and antisymmetric-coupled SPP modes in M–LC–M structure are derived and numerically solved. The effects of LC tilt angles on the effective refractive index and propagation length are proposed. The symmetric mode surface plasmons in M–LC–M structure exhibit a reduction in propagation length and enhanced field confinement by decreasing the tilt angle. The obtained analytic formula can be used as an efficient element in designing tunable ultrahigh nanoscale integrated plasmonic and optoelectronic devices.

REFERENCES

[1] Gu, J. et al.: An active hybrid plasmonic metamaterial. Opt. Mater. Express, **2** (2012), 31–37.

[2] Gao, L.; Tang, L.; Hu, F.; Guo, R.; Wang, X.; Zhou, Zh.: Active metal strip hybrid plasmonic waveguide with low critical material gain. Opt. Express, **20** (2012), 11487–11495.

[3] Kossyrev, P.A. et al.: electric field tuning of plasmonic response of nanodot array in liquid crystal matrix. Nano Lett., **5** (2005), 1978–1981.

[4] Weiss, K.; Woll, C.; Johannsmann, D.: Orientation of thin liquid crystal films on buffed polyimide alignment layers: a near-edge x-ray absorption fine structure investigation. J. Chem. Phys., **113** (2000), 11297–11305.

[5] Dorjgotov, E.A.; Bhowmik, A.K.; Bos, P.J.: High tunability mixed order photonic crystal. Appl. Phys. Lett., **96** (2010), 163507.

[6] Li, X.; Tohyama, T.; Miyashita, T.; Uchida, T.: Order parameters of the liquid crystal interface layer at a rubbed polymer surface. J. Appl. Phys., **96** (2004), 1953–1958.

[7] Werner, D.H.; Kwon, D.-H.; Khoo, I.-C.; Kildishev, A.V.; Shalaev, V.M.: Liquid crystal clad near-infrared metamaterials with tunable negative-zero-positive refractive indices. Opt. Express, **15** (2007), 3342–3347.

[8] BahramiPanah, M.; Mirtaheri, S.A.; Abrishamian, M.S.: Electrical beam steering with metal-anisotropic-metal structure. Opt. Lett., **37** (2012), 1–3.

[9] Tasolamprou, A.C.; Zografopoulos, D.C.; Kriezis, E.E.: Liquid crystal-based dielectric loaded surface plasmon polariton optical switches. J. Appl. Phys., **110** (2011), 93102-9.

[10] Dridi, M.; Vial, A.: FDTD modeling of gold nanoparticles in a nematic liquid crystal: quantitative and qualitative analysis of the spectral tunability. J. Phys. Chem. C, **114** (2010), 9541–9545.

[11] Krokhin, A.A.; Neogi, A.; McNeil, D.: Long-range propagation of surface plasmons in a thin metallic film deposited on an anisotropic photonic crystal. Phys. Rev. B, **75** (2007), 235420-5.

[12] Smolyaninov, I.I.: Two-dimensional plasmonic metamaterials. Appl. Phys. A, **87** (2007), 227–234.

[13] Jacob, J.; Babu, A.; Mathew, G.; Mathew, V.: Propagation of surface plasmon polaritons in anisotropic MIM and IMI structures. Superlattices Microstruct., **44** (2008), 282–290.

https://doi.org/10.1017/S1759078715001695 Published online by Cambridge University Press

[14] Rukhlenko, I.D.; Premaratne, M.; Agrawal, G.P.: Guided plasmonic modes of anisotropic slot waveguides. Nanotechnology, **23** (2012), 1–8.

[15] Bahramipanah, M.; Abrishamian, M.S.; Mirtaheri, S.A.: Beam manipulating by metal–anisotropic–metal plasmonic lens. J. Opt., **14** (2012), 105001-7.

[16] Maier, S.A.: Plasmonics Fundamentals and Applications, Springer, New York, 2007.

[17] Bahramipanah, M.; Abrishamian, M.S.; Mirtaheri, S.A.: Tuning the focal point of a plasmonic lens by nematic liquid crystal. J. Eur. Opt. Soc. Rapid Publ., **7** (2012), 12053-7.

[18] Ishii, S.; Kildishev, A.V.; Shalaev, V.M.; Drachev, V.P.: Controlling the wave focal structure of metallic nanoslit lenses with liquid crystals. Laser Phys. Lett., **8** (2011), 828–832.

[19] Dridi, M.; Vial, A.: FDTD modelling of gold nanoparticle pairs in a nematic liquid crystal cell. J. Phys. D: Appl. Phys., **43** (2010), 9541–9545.

[20] Liu, C.Y.; Chen, L.W.: Tunable photonic-crystal waveguide Mach–Zehnder interferometer achieved by nematic liquid-crystal phase modulation. Opt. Express, **12** (2004), 2616–2624.

[21] Chu, Y.; Schonbrun, E.; Yang, T.; Crozier, K.B.: Experimental observation of narrow surface plasmon resonances in gold nanoparticle arrays. Appl. Phys. Lett., **93** (2008), 181108-3.

[22] Guo, S.H.; Heetderks, J.J.; Kan, H.C.; Phaneuf, R.J.: Enhanced fluorescence and near-field intensity for Ag nanowire/nanocolumn arrays: evidence for the role of surface plasmon standing waves. Opt. Express, **16** (2008), 18417–18425.

[23] Seo, M.A. et al.: Terahertz field enhancement by a metallic nano slit operating beyond the skin-depth limit. Nat. Photonics, **3** (2009), 152–156.

[24] Balci, S.; Karabiyik, M.; Kocabas, A.; Kocabas, C.; Aydinli, A.: Coupled plasmonic cavities on moire surfaces. Plasmonics, **5** (2010), 429–436.

[25] Kim, D.S.; Park, H.R.; Seo, M.A.: Nanogap device for field enhancement and a system for nanoparticle detection using the same. United States Patent, Publ. No. US 2011/0220799, 2011.

Hamed Armand received his B.Sc. degree in Electrical Engineering from Shiraz University of Technology, Shiraz, Iran in 2009 and M.Sc. degree in Telecommunication Engineering from K. N. Toosi University (KNTU), Tehran, Iran in 2012. His research interests are photonic structures and anisotropic medias, metamaterial structures, and microwave circuits design.

Mansoor Dashti Ardakani received his B.Sc. degree in Electrical Engineering from Shiraz University of Technology, Shiraz, Iran in 2009 and M.Sc. degree in Telecommunication Engineering from Iran University of Science and Technology (IUST), Tehran, Iran in 2012. His current research interests include metamaterial and EBG structures, SIW structures, photonic structures, and microwave circuits design.

https://doi.org/10.1017/S1759078715001695 Published online by Cambridge University Press